RSC Advances

ROYAL SOCIETY OF CHEMISTRY

www.rsc.org/advances

Large-Area MoS_2 Thin Layers Directly Synthesized on Pyramid-Si Substrate for Surface-Enhanced Raman Scattering

Hengwei Qiu,[a] Zhen Li,[a] Saisai Gao,[a] Peixi Chen,[a] Chao Zhang,[a] Shouzhen Jiang,*[a] Shicai Xu,[b] Cheng Yang,[a] and Hongsheng Li[c]

[a]*School of Physics and Electronics, Shandong Normal University, Jinan 250014, People's Republic of China, E-mail: jiang_sz@126.com*

[b]*College of Physics and Electronic Information, Shandong Provincial Key Laboratory of Functional Macromolecular Biophysics, Institute of Biophysics, Dezhou University, Dezhou 253023, People's Republic of China*

[c]*Department of Radiation Oncology, Key Laboratory of Radiation Oncology of Shandong Province, Shandong Cancer Hospital and Institute, Jinan 250117, People's Republic of China*

Abstract

In our work, we directly synthesized few layers MoS_2 on pyramid-Si substrate to fabricate surface-enhanced Raman scattering (SERS) substrate via thermally decomposing the precursor of ammonium thiomolybdate ($(NH_4)_2MoS_4$). Scanning electron microscope (SEM), atomic force microscopy (AFM), X-ray diffraction (XRD) and Raman spectra are employed to characterize the as-grown MoS_2 layers. Adenosine and cytidine were selected as the probe molecules to investigate the SERS ability of the MoS_2-pyramid-Si substrate, has shown that the MoS_2-pyramid-Si substrate can prominently suppress photobleaching and fluorescence of the probe molecule. Compare with MoS_2-flat-Si substrate (MoS_2 layers synthesized on flat-Si substrate), the MoS_2-pyramid-Si substrate has more significant SERS ability. The minimum detected concentration of both adenosine and cytidine on MoS_2-pyramid-Si substrate can reach 10^{-6}M. Importantly, the linear relationship between Raman intensity and concentration of adenosine or cytidine can apply to the bimolecular detection. This work may provide a new opportunity for the studying of chemistry mechanism (CM) and novel SERS substrate fabricating.

1. Introduction

In recent years, SERS as a powerful tool for biomedical detection with nondestructive, ultrasensitive and real-time has attracted increasing attention.[1-3] The commonly used SERS substrates are metal nanostructures include Ag, Au, Cu and Ni in forms of nanoparticle or rough surface and semiconductors substrates include ZnO, ZnS, TiO_2, CuO, CdTe and SnO_2. However, the instability and poor biocompatibility of the metal nanoparticles have become the obstacle of the SERS substrate development.[4,5] Furthermore, the lower adsorption capacity of metal nanostructures for some molecules often limits their applications.[6] With the rapid development of the SERS technology due to its superior performance in applications, a variety of novel SERS substrates emerge in endlessly, include graphene and MoS_2.

MoS_2, which is a ultrathin 2D layered material analogous to graphene, has created great interest due to its great potential in the fields of catalysis, microelectronics, lithium batteries, hydrogen storage, dry lubricant, medical and optoelectronics.[7-13] In form, the layered MoS_2, where the Mo layer is sandwiched between two sulfur layers by covalent forces.[14] Compare with graphene, easier bio-modification of MoS_2 can be more widely used in biosensor. Recent research indicated that MoS_2 films have Raman enhancement effect, which may cause by charge transfer and dipole-dipole coupling.[15] Nowadays, the SERS substrates based on graphene or graphene-metal nanostructure have been already matured,[16-19] but the SERS substrate fabrication based on MoS_2 is still at primary stage. Importantly, MoS_2 with the high light transmission, chemical stability, biomolecular affinity and low-temperature synthesis, undoubtedly can be an ideal

platform to support SERS active. Porous Si possesses large specific area and governable nanoporous structure, which can increase the amount of the effective hot spots and further enhance the sensitivity of the SERS signals.[20-22] Recently, some groups have reported different SERS substrates based the porous Si, such as porous Si decorated with Au nanoparticles[23,24] and Ag-coated Si nanoporous.[25,26]

Here, we present a MoS_2-pyramid-Si SERS substrate with demonstrated low concentration sensitivity. Compare with graphene, large-size MoS_2 layers can be synthesized in a relatively lower temperature with relatively simple process by using thermally decomposing the precursor of $(NH_4)_2MoS_4$. Two kinds of nucleoside molecules (adenosine and cytidine) were selected to explore the SERS ability of the MoS_2-pyramid-Si substrate. The minimum detected concentration of both adenosine and cytidine can be 10^{-6}M, this undoubtedly shows the excellent Raman enhancement effect of the MoS_2-pyramids-Si substrate.

2. Experimental Section

2.1 Fabrication of MoS_2 layers

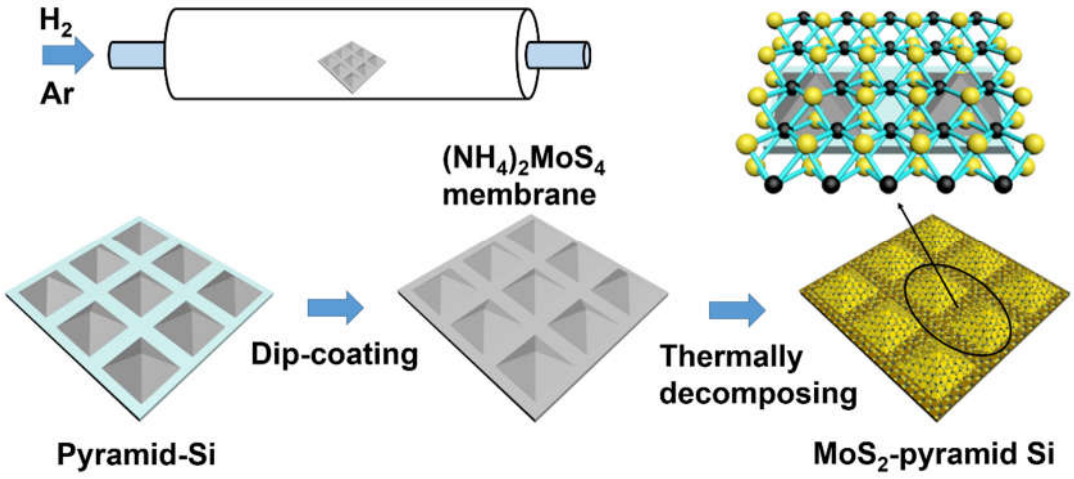

Fig.1. Schematic illustration of the process for the synthesis of MoS_2 thin layers on pyramid-Si substrates. The precursor $(NH_4)_2MoS_4$ was dip-coated on the pyramid-Si substrates. The thermally decomposing process was performed in a quartz tube furnace.

Pyramid-Si substrate (boron-doped single crystal silicon) was fabricated by using wet texturing technology with the assist of NaOH, which was described in our early work.[27] Fig.1 schematically illustrates the three steps process for the synthesis of MoS_2 thin layers. High purity of $(NH_4)_2MoS_4$ (purity of 99.99%; 1g) was dissolved in 10mL of dimethylformamide (DMF) to form a 1wt % solution. The prepared solution was ultrasonic dispersed in an ultrasonic cleaner for 20min in order to prevent undissolved particles existed. All the pyramid-Si substrates in the experiment were cleaned by acetone, alcohol and deionized water. After that the pyramid-Si substrates were immersed into the $(NH_4)_2MoS_4$ solution and spun by a spin-coater to from an ultrathin and uniform $(NH_4)_2MoS_4$ membrane. The thermally decomposing process was

performed in a quartz tube furnace and divided into three steps. First, the freshly prepared ultrathin $(NH_4)_2MoS_4$ membrane was placed in the quartz tube and the pressure was pumped to 10^{-3}pa by a double-pump system of mechanical pump and molecular pump. Second, a gas mixture (Ar: 20sccm and H_2: 80sccm) was introduced in the tube and the temperature reached 600°C for annealing 30min. After that, the tube was fast cooled down to room temperature by opening the furnace. Third, the powdered sulfur was put in the tube 30cm far from the pyramid-Si substrate. The second annealing was performed when the temperature reached 800°C with 20sccm Ar for 20min. Finally, the tube fast cooled down to room temperature again. The process of MoS_2 layers synthesized on the flat-Si substrate is similar to that on the pyramid-Si substrate, the difference here is the pyramid-Si substrate was replaced of the flat-Si substrate. In order to demonstrate the effect of the second annealing, a contrastive MoS_2-pyramid-Si (600°C) substrate was carried out. The fabrication of the MoS_2-pyramid-Si (600°C) substrate was without the second annealing of 800°C.

2.2 SERS Experiments

SERS experiments were carried out with a Horiba HR Evolution 800 Raman spectrometer with laser wavelength at 532nm. The excitation laser spot was about 0.5μm and the incident laser power was kept at 0.5mW. The laser light was coupled through an objective lens of 50× and the Raman spectra from all substrates were measured under the same conditions. All substrates were immersed in adenosine or cytidine solution with different concentrations for 2h at 25°C, washed with deionized water and dried to obtain the enhanced Raman spectra. SERS measurements were taken

from at least five random points that were more than 2mm apart. If there is no special instruction, the mentioned Raman spectra are expressed in terms of average spectra.

2.3 Apparatus and Characterization

The surface morphology of the MoS_2-pyramids-Si substrate was characterized by SEM (SEM, Zeiss Gemini Ultra-55) and AFM (Park XE-100) in the noncontact mode. The crystallinity of MoS_2 layers were characterized by XRD (Rigaku D/MAX-RB). The Raman spectra of MoS_2 film was performed using a Raman spectrometer (Horiba HR-800) with laser excitation at 532nm (2.33eV).

3. Results and discussion

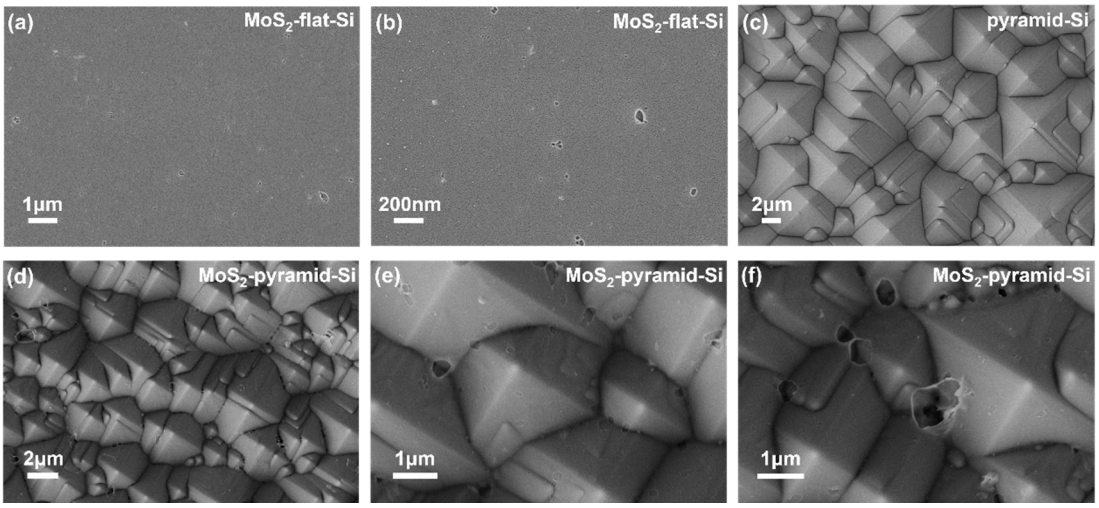

Fig. 2. (a) and (b) are SEM images of the MoS_2-flat-Si substrate in different magnification. (c) SEM image of the pyramid-Si substrate. (d), (e) and (f) are SEM images of the MoS_2-pyramid-Si substrate in different magnification.

The surface morphology of three different kinds of as-grown MoS_2 layers were evaluated by SEM image. As illustrated in the SEM images in Fig. 2(a), the MoS_2-flat-Si substrate presents a uniform color and smooth surface. In order to clearly observe the surface morphology, SEM image under a high magnification was obtained, as shown in Fig. 2(b). There are continuous cracks and few particles on the surface of the MoS_2-flat-Si substrate, indicating that uniform and complanate MoS_2 layers have complete synthetized on the flat-Si substrate. Fig. 2(c) shows the surface morphology of the pyramid-Si substrate, these regular pyramids array is relatively uniform on the pyramid-Si substrate. The average height of pyramids is 3μm and the average distance is 4μm and this porous structure can effectively improve the MoS_2 layers formation and SRES sensitivity. Fig. 2(c), Fig. 2(d) and Fig. 2(e) are SEM images of the MoS_2-

pyramid-Si substrate in different magnification. After MoS_2 layers synthetized on the pyramid-Si substrate, the substrate exhibits a darker and non-specular surface compare to the substrate without MoS_2 synthetized in Fig. 2(c). SEM images of the MoS_2-pyramid-Si substrate under a high magnification are shown in Fig. 2(d) and Fig. 2(e). Obviously, the MoS_2 thin layers almost completely covered the pyramid-Si substrate. There are few micropores on the surface of MoS_2-pyramid-Si substrate probably because some tiny bubbles were produced in the dip-coating process. Based on the above SEM images, we preliminary draw a conclusion that the MoS_2 layers have successfully synthetized on the flat-Si and pyramid-Si substrate

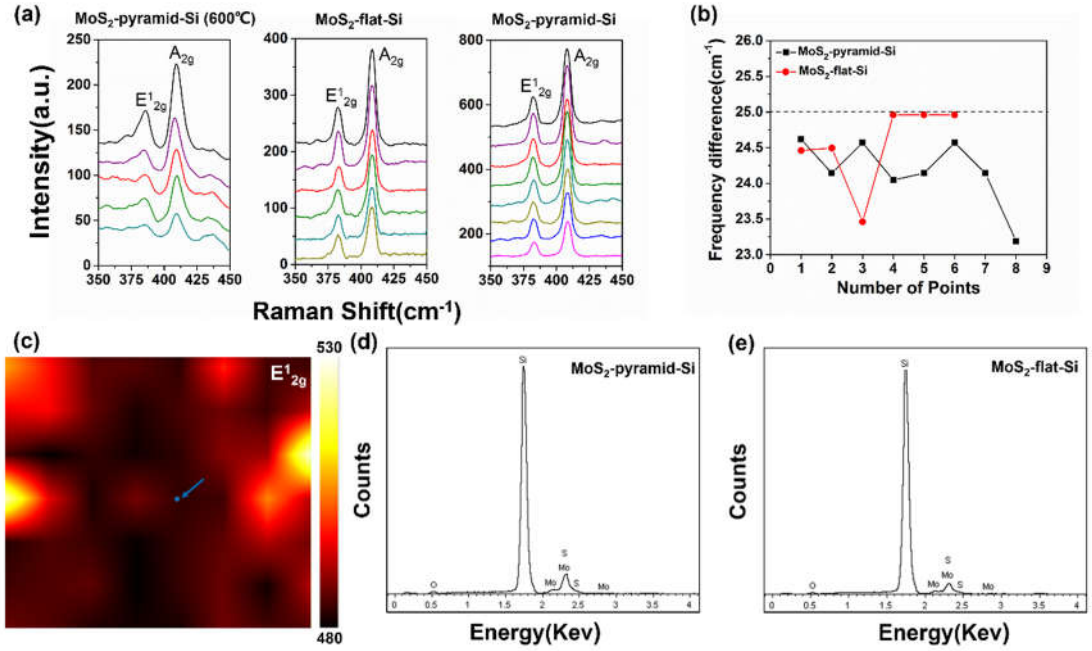

Fig.3. (a) Raman spectra of the random points obtained from the MoS_2-pyramid-Si (600°C), MoS_2-flat-Si, and MoS_2-pyramid-Si substrate. (b) The calculated peak frequency difference (Δ) between E^1_{2g} and A_{1g} Raman modes according to the Raman spectra in (a). (c) Raman mapping for the E^1_{2g} band obtained from an area of $10\times10\mu m^2$. (d) EDS spectra of the MoS_2-pyramid-Si substrate. (d) EDS spectra of the MoS_2-flat-Si substrate.

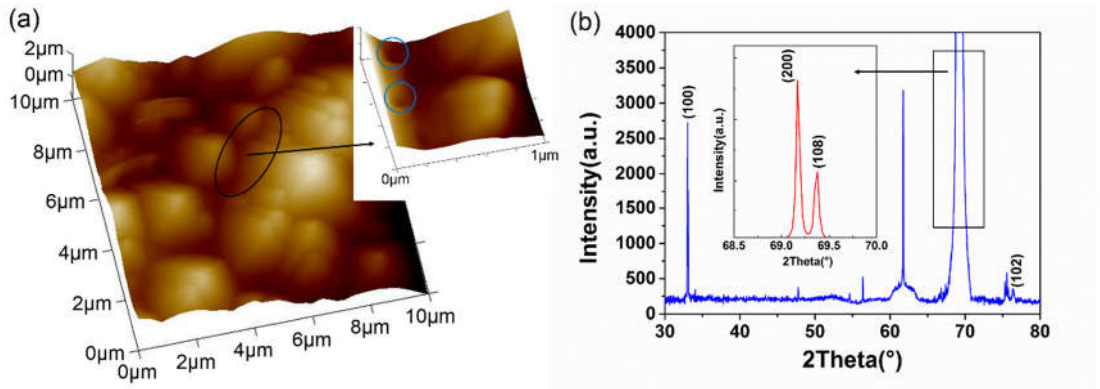

Fig. 4. (a) AFM image of the MoS_2-pyramid-Si substrate. (b) XRD pattern of the MoS_2-pyramid-Si substrate.

In order to further investigate the characteristics of the as-grown MoS_2 layers, Raman spectra were obtained from the randomly selected five points on the MoS_2-pyramid-Si (600°C) substrate, six points on the MoS_2-flat-Si substrate, and eight points on the MoS_2-pyramid-Si substrate, as shown in Fig. 3(a). For all the Raman spectra obtained from three kinds of substrates, two Raman characteristic peaks of the in-plane E^1_{2g} and the out-of-plane A_{1g} (at 360-420 cm^{-1}) vibration are all clearly seen.[28] It has been reported that the MoS_2 structure formed at the thermolysis temperature higher than 300°C. However, for the MoS_2-pyramid-Si (600°C) substrate, the relatively larger width (~10cm^{-1}) of E^1_{2g} band and weaker intensity (relative to the substrate Si peak at 520cm^{-1}) indicate that the crystal structure of MoS_2 is still not perfect. Note that the second annealing can effectively promote MoS_2 formation and sulfur source can effectively supply the sulfur vacancy. For MoS_2-flat-Si substrate and MoS_2-pyramid-Si substrate, the full-width-half-maximum (FWHM) values of E^1_{2g} and A_{1g} band respectively are 6-7 and 3-4cm^{-1}, and the stable Raman characteristic peaks indicate

that the uniform MoS_2 layers have successfully synthesized. The relatively narrow and strong of E^1_{2g} mode, which suggest the high quality of MoS_2 crystal structure. The peak frequency difference (Δ) between E^1_{2g} and A_{1g} bands can be used to identify the layer number of MoS_2.[28] The value of Δ between E^1_{2g} and A_{1g} bands obtained from the randomly selected eight points on the MoS_2-pyramid-Si substrate and six points on the MoS_2-flat-Si substrate are shown in Fig. 3(b). The eight points on the MoS_2-pyramid-Si substrate are marked with black color and the values of Δ are all in a range of 23-25cm^{-1}, which indicate that the as-grown MoS_2 are 3-5 layers. The MoS_2-flat-Si substrate are similar to the MoS_2-pyramid-Si substrate with 3-6 layers. In order to further certify the coverage rate of MoS_2 layers, Raman mapping of E^1_{2g} band was obtained from the MoS_2-pyramid-Si substrate in an area of 10×10μm^2. The blue point in Fig. 3(c) corresponds to the Raman spectra marked with blue curve in Fig. 3(a). The Raman intensity of E^1_{2g} band is in a range of 480-530 (the baseline is ~350), which indicate that the pyramid-Si substrate is almost covered with MoS_2 layers. Fig. 3(d) and Fig. 3(e) show EDS spectra from the MoS_2-pyramid-Si substrate and MoS_2-flat-Si substrate, respectively. The peaks associated to silicon element are clearly observed. The molybdenum and sulfur related peaks are very weak, possible due to the ultrathin structure of MoS_2 layers. The AFM images of the MoS_2-pyramid-Si substrate was also performed, as shown in Fig. 4(a). From the AFM image in a large-scale, one can see that the surface of the pyramid-Si array is smooth. In order to observe more clearly, a magnified AFM image was obtained, as shown in top right corner inset in Fig. 4(a). The holes marked with blue circles are correspond to the micropores in SEM images

and the depth is ~3nm (the thickness of the monolayer MoS_2 is ~0.7nm). Fig. 4(d) shows the X-ray diffraction (XRD) pattern of the MoS_2-pyramid-Si substrate, there are three pronounced peaks at 2θ=31.910°, 69.016° and 69.158° assigned as the (100), (200) and (108) reflections, respectively [powder diffraction file (PDF) no. 751539]. The (002) peak can hardly be detected, which indicate that the as-grown MoS_2 is in a structure of monolayer or few layers.[29,30]

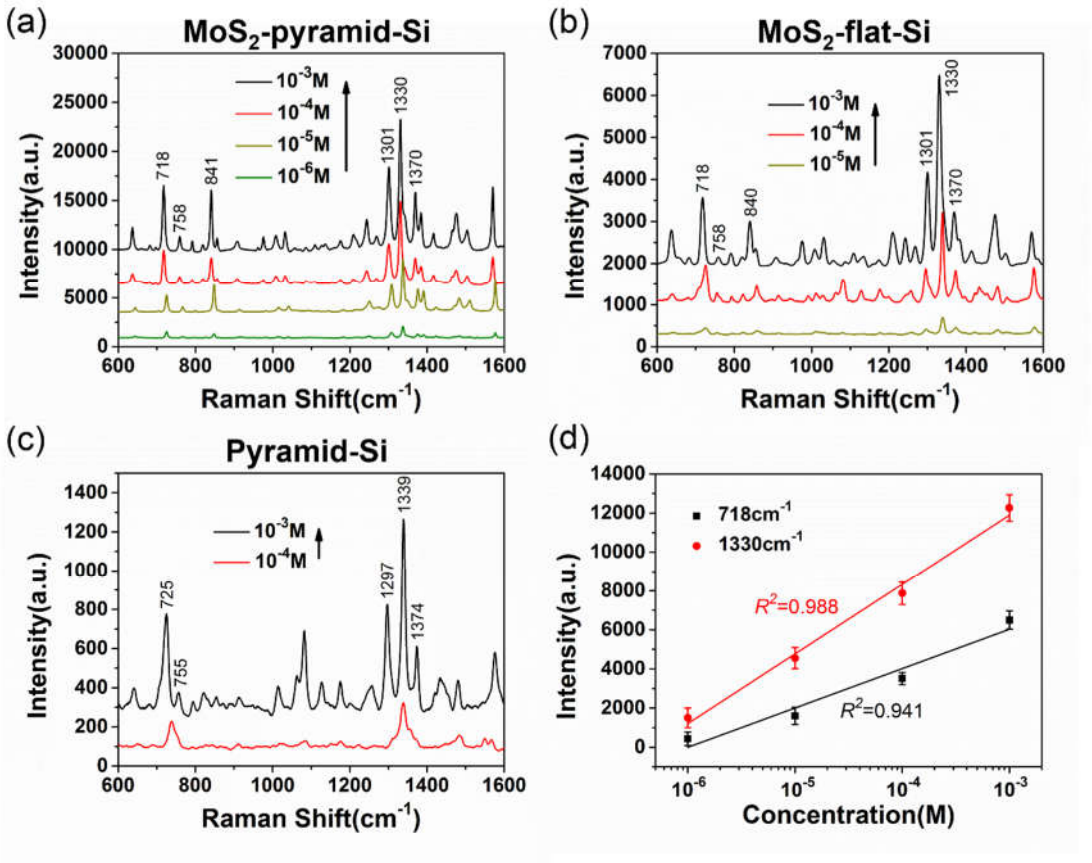

Fig.5. (a) The Raman spectra of adenosine on the MoS_2-pyramid-Si substrate from 10^{-3} to 10^{-6}M. (b) The Raman spectra of adenosine on the MoS_2-flat-Si substrate from 10^{-3} to 10^{-5}M. (c) The Raman spectra of adenosine on the pyramid-Si substrate from 10^{-3} to 10^{-4}M. (d) Raman intensity of adenosine on the MoS_2-pyramid-Si substrate at 718 and 1330cm^{-1} as a function of concentration.

Adenosine was selected as the probe molecule to demonstrate the SERS effect of the three kinds of substrate. The characteristic Raman peaks of adenosine have confirmed according to the previous works.[31,32] The peaks at 725 and 1576cm^{-1} assigned to the ring breathing modes of the whole molecule. The peak at 841cm^{-1} assigned to skeletal mode of C-O-C. The peak at 1301cm^{-1} assigned to the stretching vibration of N-C-N and C-C-N. The peak at 1330cm^{-1} assigned to the stretching vibration of C-N and the bending vibration of C-H. The peak at 1370cm^{-1} assigned to the bending vibration of N-H and C-H. For all the SERS substrates, the measured Raman intensity decay with the decrease of the adenosine concentration. As shown in Fig. 5(a) and Fig. 5(b), the minimum detected concentration of adenosine from MoS_2-pyramid-Si substrate is one order of magnitude lower than that from MoS_2-flat-Si substrate, which can be as low as 10^{-6}M. This enhancement effect is almost reached the detection limit of Ag-Si pillar array (adenine of 10^{-6}M) and Ag-Si pyramid (adenosine of 10^{-7}M).[25,27] The Raman intensity from MoS_2-pyramid-Si substrate is 3-5 times stronger than that from MoS_2-flat-Si substrate, which can attributed to the well-separated pyramid arrays. The pyramid-Si arrays can effectively make the incident laser oscillate between the pyramidal valleys, which will further lead to local enhancement of the incident laser. The scattering area of MoS_2-pyramid-Si substrate is relatively larger than MoS_2-flat-Si substrate, which can further enhance the scattering cross-section. Fig. 5(c) shows the Raman spectra of adenosine obtained from pyramid-Si substrate and the minimum detected concentration only reached 10^{-4}M. This phenomenon can be due to the lack of surface plasmons and only this local

enhancement of the incident laser can't support the SERS active. Compare the Raman spectra from MoS_2-pyramid-Si substrate with that from pyramid-Si substrate, more effective enhancement effect is obvious. The peaks at 718 (725) cm^{-1} from MoS_2-pyramid-Si substrate is ~13.2 times stronger than that from pyramid-Si substrate. The peaks at 1301 (1297) cm^{-1} from MoS_2-pyramid-Si substrate is ~15.6 times stronger than that from pyramid-Si substrate. The peaks at 1330 (1339) cm^{-1} from MoS_2-pyramid-Si substrate is ~13.5 times stronger than that from pyramid-Si substrate. The enhancement factors for other peaks are relatively weaker than the peaks above mentioned. From the comparison, the enhancement factors for different peaks are about in a range of 2-15. It should be noted that the multiple of the enhancement, 2-15 times and the vibration dependence of the enhancement factors are both consistent with the chemical enhancement mechanism. Moreover, for pyramid-Si substrate with the concentration of 10^{-4}M, some Raman peaks can't be distinguished because of the merger phenomena, such as the peaks at 725 and 755cm^{-1}, which indicates that MoS_2 layers can contribute to the peak identification. The Raman peaks from MoS_2-pyramid-Si substrate appear little red shift or blue shift compare with that from pyramid-Si substrate, which is because the chemical interaction of charge transfer and dipole-dipole coupling. The peaks at 718 and 1330cm^{-1} were selected to investigate the relationship between the Raman intensity and the concentrations. Fig. 5(d) shows the Raman intensity as a function of the adenosine concentrations. To represent the capability of the quantitative detection of adenosine, the linear fit calibration curve (R^2) with error bars is presented and the value of R^2 of 718 and 1330cm^{-1} can reach 0.941 and 0.988,

respectively. The excellent linear response between the Raman intensity and adenosine concentrations prove that the prepared MoS_2-pyramid-Si substrate can serve as good SERS substrate for nucleoside detection.

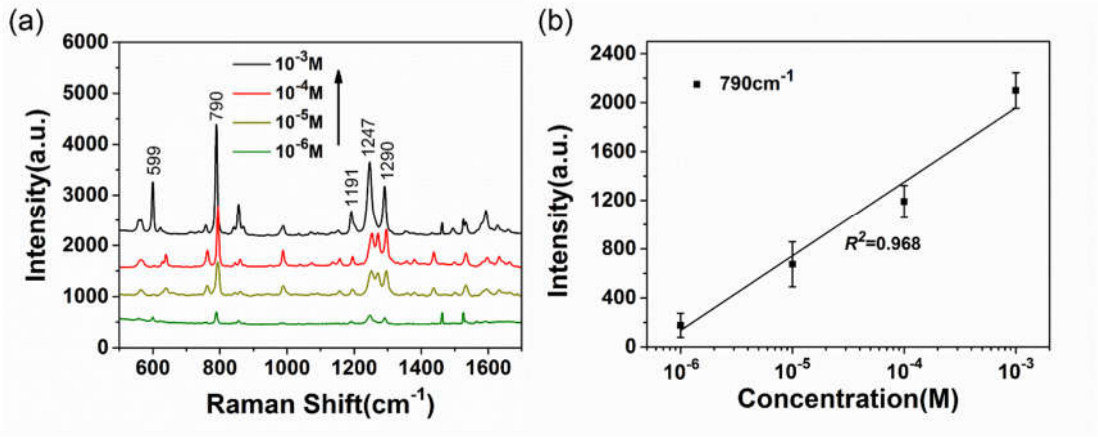

Fig.6. (a) The Raman spectra of cytidine on the pyramid-Si substrate from 10^{-3} to 10^{-6}M. (b) Raman intensity of cytidine on the MoS_2-pyramid-Si substrate at 790cm^{-1} as a function of concentration.

In order to further demonstrate the feasibility of the prepared SERS substrate for nucleoside detection, another nucleoside molecule was selected in experiment, which is cytidine. As shown in Fig. 6(a), all the Raman peaks are inosculate with the reported work.[33,34] The peak at 599cm^{-1} assigned to the deformation ring. The peak at 790cm^{-1} assigned to the ring breathing. The peaks at 1247 and 1290cm^{-1} assigned to stretching vibration of C-N and bending vibration of N-H and C-H. There are different enhancement effect of each Raman peak due to the different adsorption states, such as the peak at 599cm^{-1} is noticeable for concentration of 10^{-3}M and negligible for concentration of 10^{-4}-10^{-6}M. The peak at 1270cm^{-1} is just opposite with the peak at 599cm^{-1}. The Raman intensity of the peaks at 790cm^{-1} shows the close relationship with the concentrations of cytidine, which was selected to further study the enhancement

effect. Fig. 6(b) shows the reasonable linear response between the Raman intensity and the concentration of cytidine, the value of R^2 is reached 0.968, which indicates the as-grown MoS_2-pyramid-Si substrate is an effective platform for the SERS molecular detection. The MoS_2 layers cover metal nanoparticles may have better Raman enhancement effect, further studies are now in progress in our group.

4. Conclusions

We have successfully synthesized MoS_2 thin layers on the pyramid-Si substrate for SERS detection. Two different nucleoside molecules (adenosine and cytidine) were selected to investigate the SERS ability of the papered substrate, show that the MoS_2-pyramid-Si substrate possesses excellent Raman enhancement effect. The minimum detected concentration of both adenosine and cytidine can be as low as 10^{-6}M, which can be attributed to the biological compatibility and chemical enhancement of MoS_2. This MoS_2-pyramid-Si substrate may provide a new way toward practical applications for the ultrasensitive and label-free SERS detection of biomolecule. The combination of MoS_2 and metal nanoparticles is now in progress in our group.

Acknowledgments

The authors are grateful for financial support from the National Natural Science Foundation of China (61205174, 61401258, 11404193, and 11474187), Shandong Province Natural Science Foundation (ZR2013HL049, ZR2013EMM009, and ZR2014FQ032), and Excellent Young Scholars Research Fund of Shandong Normal University.

References

[1] S. Nie and S.R. Emory, *Science*, 1997, **275**, 1102-1106.

[2] A. Barhoumi and N.J. Halas, *J. Am. Chem. Soc.*, 2010, **132**, 12792-12793.

[3] K. Lee, V.P. Drachev and J. Irudayaraj, *ACS Nano*, 2011, **5**, 2109-2117.

[4] X. Ling, L.M. Xie, Y. Fang, H. Xu, H.L. Zhang, J. Kong, M.S. Dresselhaus, J. Zhang and Z.F. Liu, *Nano Lett.*, 2010, **10**, 553-561.

[5] Y.M. Liu, Y. Hu and J. Zhang, *J. Phys. Chem. C*, 2014, **118**, 8993-8998.

[6] J. Zheng, X. Li, R. Gu and T. Lu, *J. Phys. Chem. B*, 2002, **106**, 1019-1023.

[7] Y.G. Li, H.L. Wang, L.M. Xie, Y.Y. Liang, G.S. Hong and H.J. Dai, *J. Am. Chem. Soc.*, 2011, **133**, 7296-7299.

[8] B. Radisavljevic, A. Radenovic, J. Brivio, V. Giacometti and A. Kis, *Nat. Nanotechnol.*, 2011, **6**, 147-150.

[9] J. Xiao, D Choi, L. Cosimbescu, P. Koech, J. Liu and J.P. Lemmon, *Chem. Mater.*, 2010, **22**, 4522-4524.

[10] H. Hwang, H. Kim and J. Cho, *Nano Lett.*, 2011, **11**, 4826-4830.

[11] L.F. Sun, J.X. Yan, D. Zhan, L. Liu, H.L. Hu, H. Li, B.K. Tay, J.L. Kuo, C.C. Huang, D.W. Hewak, P.S. Lee and Z.X. Shen, *Phys. Rev. Lett.*, 2013, **111**, 126801.

[12] H. Wang, L.L. Yu, Y.H. Lee, Y.M. Shi, A. Hsu, M.L. Chin, L.J. Li, M. Dubey, J. Kong and T. Palacios, *Nano Lett.*, 2012, **12**, 4674-4680.

[13] Q.J. Xiang, J.G. Yu and M. Jaroniec, *J. Am. Chem. Soc.*, 2012, **134**, 6575-6578.

[14] J.L. Verble and T.J. Wieting, *Phys. Rev. Lett.*, 1970, **25**, 362-365.

[15] X. Ling, W.J. Fang, Y.H. Lee, P.T. Araujo, X. Zhang, J.F. Rodriguez-Nieva, Y.X.

Lin, J. Zhang, J. Kong and M.S. Dresselhaus, *Nano Lett.*, 2014, **14**, 3033-3040.

[16] P. Wang, O. Liang, W. Zhang, T. Schroeder and Y.H. Xie, *Adv. Mater.*, 2013, **25**, 4918-4924.

[17] W.G. Xu, J.Q. Xiao, Y.F. Chen, Y.B. Chen, X. Ling and J. Zhang, *Adv. Mater.*, 2013, **25**, 928-933.

[18] Y.W. Zhang, S. Liu, L. Wang, X.Y. Qin, J.Q. Tian, W.B. Lu, G.H. Chang and X.P. Sun, *RSC Advances*, 2012, **2**, 538-545.

[19] S.C. Xu, B.Y. Man, S.Z. Jiang, J.H. Wang, J. Wei, S.D. Xu, H.P. Liu, S.B. Gao, H.L. Liu, Z.H. Li, H.S. Li and H.W. Qiu, *ACS Appl. Mater. Interfaces*, 2015, **7**, 10977-10987.

[20] A. Chiolerio, A. Virga, P. Pandolfi, P. Martino, P. Rivolo, F. Geobaldo and F. Giorgis, *Nanoscale Res. Lett.*, 2012, **7**, 1-7.

[21] Y.Q. Wang, S. Ma, Q.Q. Yang and X.J. Li, *Appl. Surf. Sci.*, 2012, **258**, 5881-5885.

[22] B. Kiraly, S. Yang and T.J. Huang, *Nanotechnology*, 2013, **24**, 245704.

[23] X. Sun, N. Wang and H. Li, *Appl. Surf. Sci.*, 2013, **284**, 549-555.

[24] J.Q. Li, C. Chen, H. Jans, X.M. Xu, N. Verellen, I. Vos, Y. Okumura, V.V. Moshchalkov, L. Lagaea and P.V. Dorpe, *Nanoscale*, 2014, **6**, 12391-12396.

[25] F. Feng, G. Zhi, H.S. Jia, L. Cheng, Y.T. Tian and X.J. Li, *Nanotechnology*, 2009, **20**, 295501.

[26] R.R. Juluri, A. Rath, A. Ghosh, A. Bhukta, R. Sathyavathi, D.N. Rao, K. Muller, M. Schowalter, K. Frank, T. Grieb, F. Krause, A. Rosenauer and P.V. Satyam, *Sci. Rep.*, 2014, **4**, 4633.

[27] C. Zhang, B.Y. Man, S.Z. Jiang, C. Yang, M. Liu, C.S. Chen, S.C. Xu, H.W. Qiu and Z. Li, *Appl. Sur. Sci.*, 2015, **347**, 668-672.

[28] C. Lee, H. Yan, L.E. Brus, T.F. Heinz, J. Hone and S. Ryu, *ACS nano*, 2010, **4**, 2695-2700.

[29] K.F. Mak, C. Lee, J. Hone, J. Shan and T.F. Heinz, *Phys. Rev. Lett.*, 2010, **105**, 136805-1-4.

[30] H.S.S. Ramakrishna Matte, A. Gomathi, A.K. Manna, D.J. Late, R. Datta, S.K. Pati and C.N.R. Rao, *Angew. Chem. Int. Ed.*, 2010, **49**, 4059-4062.

[31] B. Giese and D. McNaughton, *Phys. Chem. B*, 2002, **106**, 101-112.

[32] J. Li and Y. Fang, *Spectrochim. Acta Part A*, 2007, **66**, 994-1000.

[33] J.S. Suh and M. Moskovit, *J. Am. Chem. Soc.*, 1986, **108**, 4711-4718.

[34] S. Mansya, W.L. Peticolasa and R.S. Tobias, *Spectrochim. Acta Part A*, 1979, **35**, 315-329.